Proton Diffusion Determination and Dual Structure Model for Nickel Hydroxide Based on Potential Step Measurements on Single Spherical Beads

Liang Xiao,[†] Jun-tao Lu,[†] Pei-fang Liu,[†] Lin Zhuang,*[,†] Jiawei Yan,[‡] Yonggang Hu,[‡] Bingwei Mao,[‡] and Changjian Lin[‡]

Department of Chemistry, Wuhan University, Wuhan 430072, China, and Department of Chemistry and State Key Laboratory for Physical Chemistry of the Solid Surfaces, Xiamen University, Xiamen 361005, China

Received: September 11, 2004; In Final Form: December 4, 2004

Potential step measurement is carried out on single beads of spherical nickel hydroxide to determine the proton diffusion coefficient (*D*) and concentration of the effective proton vacancies (*C*). The semi-infinite diffusion equation for the initial stage and the finite diffusion equation for the long-term of the current response to potential step are used for deducing the *D* and *C* values. The diffusion coefficients deduced from short and long-term current responses are in the order of magnitude 10^{-7} and 10^{-10} cm^2 s^{-1}, respectively. The sum of the effective proton vacancy concentrations associated with the two *D* values comes out to be equal within experimental error to the effective proton vacancy concentration converted from the released electricity during discharge. A dual structure model is proposed to interpret the above-mentioned findings, featuring densely packed grains within which proton diffusion is slow and an inter-grain matrix where proton diffusion is fast. With this model the huge difference (about 6 orders of magnitude) in *D* values reported in the literature as well as the controversy of the dependence of diffusion coefficient on the state of charge can be largely rationalized. This dual structure model is supported by SEM and AFM observations.

1. Introduction

Nickel hydroxide is the active material for the positive electrode of several rechargeable battery systems, including nickel/cadmium, nickel/hydrogen, nickel/metal hydrides, and nickel/zinc.[1] The charge/discharge process of nickel hydroxide involves a release/uptake of proton:

$$Ni(OH)_2 \leftrightarrow NiOOH + H^+ + e^-$$

It is generally recognized that both the charge and discharge processes are mainly controlled by the solid-state diffusion of protons in the active material.[2−4] The diffusion coefficient of protons (or equivalently the diffusion coefficient of proton vacancies) is of obvious importance for the battery performance, especially for high power density batteries such as those for electrical vehicles. Therefore, the problem of proton diffusion in nickel hydroxide has attracted much attention. The works on the proton diffusion coefficient for nickel hydroxide, including its determination and implication on electrode performance, have been excellently reviewed and reference papers before the year of 2000 can be found from that review.[5]

The main techniques used for determining the proton diffusion coefficient, *D*, in nickel hydroxide include cyclic voltammetry,[6,7] potential step,[7−12] and electrochemical impedance spectroscopy.[13] The proton diffusion coefficient had been experimentally determined for samples made in different ways. Some authors reported the *D* value obtained from electrochemical measurements on practical porous electrodes made from powder nickel hydroxide.[14] These reported values were affected more or less by the complicated porous structure of the electrode. In contrast, the results based on the measurements on deposited thin layers or single particles of nickel hydroxide could be considered essentially intrinsic for the material. However, even with these samples the reported *D* values were widely scattered, from the order of about 10^{-7} to 10^{-13} cm^2 s^{-1}. A number of possible causes were suggested by different authors for the difference in reported *D* values. For example, Ta and Newman put forward either possible reasons and reviewed a few of representative works in detail.[11] The suggested possible reasons included the *D* dependence on the state of charge (SOC), the difference in sample preparation and other experimental conditions such as the roughness factor of the substrate and cracks in the deposited films, oxygen evolution, etc. However, the unusually large scattering of the *D* value remains an open question.

Besides the *D* value, the effective concentration of protons (or the proton vacancies), *C*, in the material is as important but was ignored in previous papers reporting *D* determinations. The effective concentration here refers to the concentration of protons (or proton vacancies) participating in the charge and discharge processes. It is well-known that the utilization of the active material in batteries is usually less than unity, implying only a part of the protons that are supposed to be active in the molecular formula is really active in charging and discharging processes. Therefore, the term ΔC in diffusion equations should be the change of the effective concentration instead of the formal concentration indicated by the molecular formula. In principle, it is possible to obtain both *D* and ΔC by transient electrochemical measurements. For example, in potential step measurements, the slope of the logarithmic current vs time for the long-term current response provides the *D* value without the need for a known ΔC provided the thickness of a film or the radius of a spherical bead is known. The ΔC value can then be found from thus obtained *D* and the intercept of the straight line. This

* Corresponding author. E-mail: lzhuang@public.wh.hb.cn, Fax: +86-27-68754067.
[†] Wuhan University.
[‡] Xiamen University.

10.1021/jp045888i CCC: $30.25
Published on Web 02/12/2005

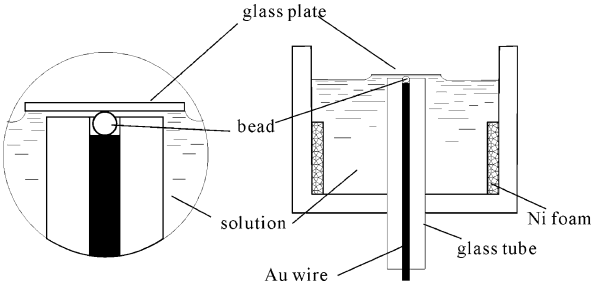

Figure 1. Cell design.

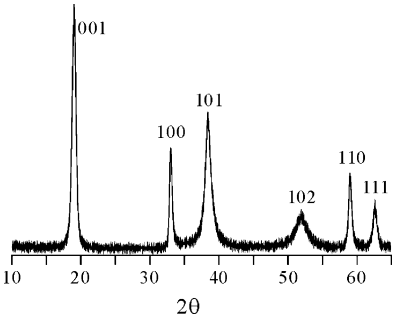

Figure 2. XRD of spherical nickel hydroxide.

approach is applicable to both thin films and spherical beads. In the short term (the initial stage) of response to a potential step, the current is linear with respect to the reciprocal of the square root of time. For film samples, the straight line goes through the origin and the diffusion coefficient can be deduced from the slope with a ΔC value obtained from other methods (often estimated based on a measured density and the molecular formula, assuming unity utilization).

In comparing with film samples, single spherical samples are advantageous because the straight line of current vs $t^{-1/2}$ will have a nonzero intercept, enabling one to deduce both D and ΔC (see eqs 1 and 2 below). Another advantage of a spherical sample for the study of proton diffusion is the fact that the dimension of a spherical sample can be easily measured under an optical microscope. In contrast, the thickness of a deposited thin film of nickel hydroxide is much more difficult to measure and in the literature the film thickness was often estimated indirectly, for example, from the electric charge consumed in deposition with assumed current efficient (usually assumed to be unity) and the density of the deposit. Moreover, spherical nickel hydroxide is the currently prevailing form of nickel hydroxide for battery manufacturing because it allows higher packing density than other forms of nickel hydroxide materials. Therefore, it is of both academic and technical significance to study the proton diffusion within spherical nickel hydroxide using the single bead approach.

Kim and co-workers first reported electrochemical measurements on single beads of spherical nickel hydroxide.[12] In their work, a carbon fiber was used to contact electronically with a single bead (a particle) so that the bead acted as the working electrode. On the basis of the radius measured under a microscope and the long-term current response to a potential step, they reported D values around $(3-4) \times 10^{-9}$ cm^2 s^{-1} without appreciable dependence on SOC, but no attempt was made to deduce C.

In the present work, potential step measurements on single beads of spherical nickel hydroxide were conducted using the microcavity electrode technique. A large amplitude cathodic potential step was applied to a charged single bead and both D and C values were deduced from the long-term as well as the initial current responses. A dual structure model was proposed to interpret these results. Atomic force microscope (AFM) and scanning electron microscope (SEM) observations were carried out to verify the proposed model.

2. Experimental Section

A gold microdisk electrode (30 μm in diameter) was anodically etched in 8 mol L^{-1} HCl to form a cavity about 20 μm deep at the tip. The microelectrode was held in position as shown in Figure 1 by the screw mechanism used in mechanical pencils (not shown). A nickel hydroxide bead (ranging 20−30 μm in diameter) was moved into the cavity with a piece of glass fiber under a stereomicroscope (120×), about one-third of the height of the bead exposed over the terminal plane of the glass tube. A piece of cover glass for microscopy was placed on top of the bead, and an appropriate force was applied on the glass piece to ensure a good electrical contact between the bead and the gold substrate (the bottom of the microcavity). The required force was realized by the surface tension of the solution meniscus (as shown in the insert of Figure 1) or by a specially designed finely tunable mechanism. The diameter of the bead was measured under a metallographic microscope (640×). A piece of nickel foam about 0.2 cm^2 (apparent area) was used as the reference and counter electrode. The potential is reported in this paper with respect to the reversible hydrogen electrode in the same solution (5 mol L^{-1} KOH). All experiments were carried out at room temperature on an electrochemical analyzer (CHI634a, Shanghai Chenhua Instruments).

Spherical nickel hydroxide samples from different commercial sources were tested in this work. These samples contained Co and other additives. Though the composition differed slightly from one to another, their experimental diffusion coefficients turned out to be essentially the same. The true density of the material was measured using a pycnometer filled with water and found to be 3.7 g cm^{-3}. The X-ray diffraction (XRD) of all these samples showed a characteristic pattern of β-Ni(OH)$_2$ (Figure 2).

The nickel hydroxide as received was green and semitransparent. As generally recognized, the green nickel hydroxide has poor electronic conductivity. In our experiments, the green beads were first fully charged (electrochemically oxidized) to black to become electronically conductive. A cathodic potential step was than applied to the black bead. At the end of cathodic potential step, the bead remained essentially black. The current response to the potential step was found to obey fairly well the diffusion equations for short- and long-term responses, indicating that the electronic conductivity in the bead was adequate for the transient measurements. Before potential step measurements, the single bead was kept at 1.45 V (vs RHE) for 1 h after full charge to reach a pseudo-equilibrium distribution of protons in the bead. Then the potential was stepped to 1.15 V (except for the stair-wise discharge) and the response current was recorded for 1000 s with sampling frequency 30 points per second.

Tapping mode AFM measurements were carried out on a SPIP AFM device which was quipped with an optical microscope for locating the AFM tip to the area to be detected. In this work the optical microscope functioned also as a bridge between AFM and SEM, enabling one to observe exactly the same area by the two techniques. The samples for microscopic studies were the nickel hydroxide beads fixed in a mixture of graphite powder and epoxy resin. The purpose of adding graphite was to endow the mixture with the electric conductivity necessary for SEM. The surface to be examined was either the

cleavage surface of a bead or the cross section of a bead polished with fine metallographic polishing paper. To compare AFM with SEM, a sample was first examined with AFM and then sputtered with a very thin layer of gold and observed with SEM.

3. Results and Discussion

3.1. Two Sets of *D* and *C* Values Deduced from Potential Step Measurements. In the potential step measurement, the potential changed from 1.45 V, where the sample bead was fully charged, to 1.15 V, where the surface of the bead was fully discharged. To prevent the possible interference of oxygen evolution, only cathodic potential step was performed for the deduction of *D* and *C* values in this work. Because the amplitude of the step was large, the kinetics of charge transfer reaction was sufficiently fast so that the current response was governed by the diffusion of protons from the bead surface into the bead body. However, at lower temperatures (10 °C or below) the slow kinetics would distort the current response. Since the activation energy for proton diffusion in nickel hydroxide is small,[10,14] the potential step measurement was carried out at room temperature (24 ± 3 °C) without using a thermostat. According to the equations for the diffusion into or out from spherical bodies, in the initial domain the current response can be well approximated by a linear equation of $t^{-1/2}$ (eq 1) while for the long time domain, the current decreases exponentially with time to a good approximation (eq 2):[15]

$$i = 4nF\,\pi r^2\,D\Delta C\left(\frac{1}{\sqrt{\pi Dt}} - \frac{1}{r}\right) \tag{1}$$

$$i = 8nF\,\pi rD\Delta C\,\exp[(-\pi^2 D/r^2)t] \tag{2}$$

where *F* is the Faraday constant, *r* is the radius of the spherical body, ΔC is the variation of the surface concentration caused by the potential step for the diffusing species, *n* is the number of electrons involved in the reaction, and $n = 1$ for the system under study. In the charge and discharge of nickel hydroxide, the diffusing species are protons. However, the problem of proton diffusion can be treated equivalently as the problem of proton vacancy diffusion in mathematics. The latter is more convenient because the effective proton vacancy concentration is more straightforwardly correlated to releasable electricity stored in a charged bead. In the text below, the terms "diffusion of protons" and "diffusion of proton vacancies" are used interchangeably. After a large cathodic potential step the surface concentration of the effective proton vacancies can be taken as zero, i.e., the surface concentration change ΔC due to the large potential step is equal to the original bulk concentration *C* of the effective proton vacancies in a charged bead. In this way, the ΔC in eqs 1 and 2 can be replaced by the bulk concentration of the effective proton vacancies *C* in the charged state:

$$i = 4nF\,\pi r^2\,DC\left(\frac{1}{\sqrt{\pi Dt}} - \frac{1}{r}\right) \tag{1A}$$

$$i = 8nF\,\pi rDC\,\exp[(-\pi^2 D/r^2)t] \tag{2A}$$

Figure 3 shows that the current response followed eq 1A fairly well in the initial stage after the potential step. A slight bend of the line may be attributed to the kinetic sluggishness compared with the large diffusion rate at the very beginning of the potential step. On the whole, the data points in Figure 3 can be fitted to a good approximation by a straight line with an intercept *A* and a slope *B*. By comparing the plot with eq 1A, two equations are obtained:

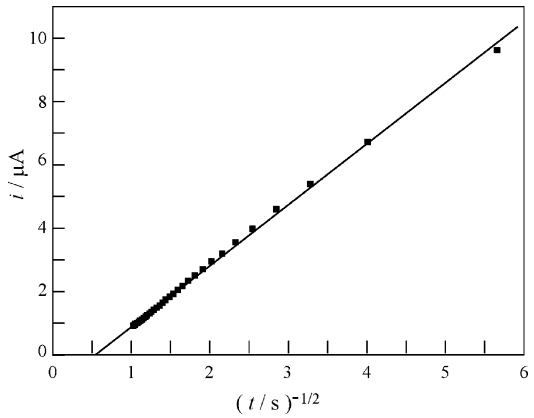

Figure 3. Initial stage response.

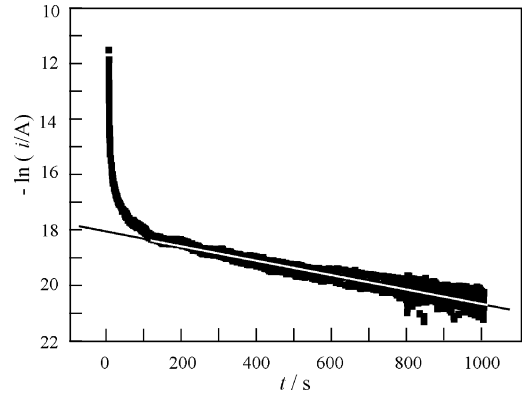

Figure 4. Long-term response.

TABLE 1: Typical Data for the Potential Step Measurement on a Single Bead

D_f, 10^{-7} $cm^2\,s^{-1}$	C_f, mol cm^{-3}	D_s, 10^{-10} $cm^2\,s^{-1}$	C_s, mol cm^{-3}	C_Σ, mol cm^{-3}	C_T, mol cm^{-3}	$1 - C_\Sigma/C_T$
1.88	0.006 48	6.08	0.0162	0.0227	0.0229	0.014
1.91	0.006 36	8.53	0.0173	0.0236	0.0234	−0.0079
2.07	0.006 34	9.88	0.0174	0.0237	0.0240	0.0135

$$A = -4F\pi rDC \tag{1A-a}$$

$$B = 4F\pi^{1/2}r^2D^{1/2}C \tag{1A-b}$$

In eqs 1A-a and 1A-b, *A*, *B*, and *r* are experimentally accessible values and *n* has been omitted because $n = 1$. The two grouped equations are independent to each other mathematically and contain two common unknown values *D* and *C*. By solving these equations, both *D* and *C* can be deduced.

Figure 4 shows that a good linearity predicated by eq 2A was obtained beyond 200 s after the potential step. The plot of ln(*i*) vs *t* produces an intercept *a* and a slope *b*, and according to eq 2A, they are related to *D* and *C* by the following equations:

$$a = \ln(8F\pi rDC) \tag{2A-a}$$

$$b = -\pi^2 D/r^2 \tag{2A-b}$$

Similar to the situation of eqs 1A-a and 1A-b, another set of *D* and *C* values can be obtained by solving the grouped eqs 2A-a and 2A-b.

To give an example, Table 1 shows the data obtained in successive three measurements on a bead of 16.7 μm radius. The *D* values from the short term (D_f, the subscript f stands for

"fast") came out to be larger by about 3 orders of magnitude than those from the long-term (D_s, the subscript s stands for "slow"). In over 30 measurements on samples from 4 suppliers, the averaged D_f and D_s were $(1.85 \pm 1.53) \times 10^{-7}$ and $(6.00 \pm 4.33) \times 10^{-10}$ cm^2 s^{-1}, respectively. It was found that the difference between individual beads from the same supplier was comparable to that between suppliers. Therefore, we shall disregard the difference of sample sources in the discussion below and focus on the interpretation of the difference in the order of magnitude for the diffusion coefficients obtained from single bead measurements. In the literature, most researchers reported only a single D value for a sample or SOC independent D values. Only a few papers reported SOC dependent D values. Motupally and co-workers[13] carried out ac impedance measurements on cathodically deposited nickel hydroxide films and found D values changing with SOC from 3.4×10^{-8} to 6.4×10^{-11} cm^2 s^{-1}; Yoon and co-workers[8] also reported D values changing over about the same orders of magnitude. In contrast, Ta and Newman[11] reported D values changing with SOC over only about an order of magnitude (1.9×10^{-12} to 2×10^{-13} cm^2 s^{-1}).

3.2. Approximate Equality of C_T and C_Σ. After two very different D values were obtained experimentally, it was natural to ask whether they were the D values corresponding to different SOC values for a single homogeneous phase or they belonged to two different components (two different forms of nickel hydroxide) coexisting in a single bead, each with its own SOC independent D. One way to check that point is to compare the corresponding C (the effective concentration of proton vacancies in the fully charged bead) values. If the two C values corresponding to the two D values were equal to each other within experimental error, the first case might be true. As shown in Table 1, the values of C_f and C_s are not the same, differing by a factor of about 3, indicating the possibility of two different components in coexistence. If the active material of the bead consisted mainly of these two components, the sum of the two concentrations, $C_\Sigma = (C_f + C_s)$, should be close to the total effective proton vacancy concentration at the fully charged state, C_T. A comparison of C_Σ and an independently obtained C_T would be very useful in this regard. The C_T value can be found from the bead volume and the total dischargeable capacity (the releasable charge, Q_T) according to Faraday's law:

$$C_T = 3Q_T/4F\pi r^3 \quad (3)$$

During the potential step measurement, the electricity released in the 1000 s of recording time, Q_{1000}, accounts for the most of the releasable charge stored in the bead. The value of Q_{1000} can be easily found by integrating the recorded transient current over the time interval of 1000 s. However, there was still a small amount of releasable charge left in the bead by the end of the potential step measurement. This residual charge can be calculated by extrapolating the experimental data. As shown by eq 2A and verified by Figure 4, in the long term, the current decays with time exponentially. It means that if the potential step measurement continued to infinite time, the current would decay according to the following equation:

$$i = \exp(a) \exp(bt) \quad (4)$$

a and b are the intercept and slope, respectively, of the linear fitting shown in Figure 4. Note that b is negative and the integration of eq 4 from $t = 1000$ s to infinite time results in a finite value $[\exp(a) \exp(-1000b)]/(-b)$ which is the residual releasable charge, Q_{res}, and was found to account for a few percentages of the total releasable charge, varying from bead to bead. In Table 1, C_T is the total concentration of effective proton vacancies converted from the total releasable charge using eq 3, where $Q_T = (Q_{1000} + Q_{res})$.

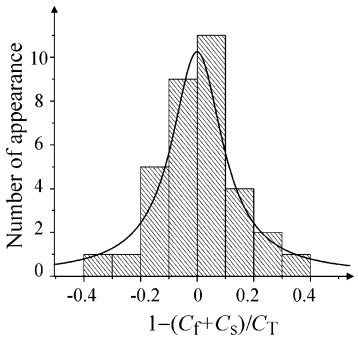

Figure 5. Statistics of $1 - (C_f + C_s)/C_T$ over 34 measurements on 18 beads from 4 suppliers.

As shown in Table 1, the independently obtained C_T and C_Σ are indeed approximately equal to each other, $C_T \approx C_\Sigma$, supporting the assumption of two different coexisting forms of nickel hydroxide in the bead. The approximate equality was further proved by more experimental data. Figure 5 shows the statistics of 34 measurements on 18 beads from 4 suppliers, showing that the data points of $(1 - C_\Sigma/C_T)$ follow quite well the Gauss distribution law and the mean is very close to zero (mean $= -0.00014$, standard deviation $= 0.147$).

This approximate equality has profound significance, indicating that there are two independent components in a single bead with different SOC independent diffusion coefficients and different effective proton vacancy concentrations. The fast diffusing component is predominant in the initial response of the potential step measurement while the slow one overwhelming in the long term. The two proton vacancy concentrations both contribute to the discharge capacity, therefore the sum of the two concentrations is equal to the total concentration of the effective proton vacancies converted from the discharge capacity.

3.3. Dual Structure Model. *3.3.1. Qualitative Description of the Model.* All previously published works on the determination of proton diffusion coefficient in nickel hydroxide adopted a homogeneous model even though substructures in the material were realized by some of the authors. Yoon and Pyun[8] discussed the proton transport in nickel hydroxide with a proton trap model in which the concentration of proton traps and release rate of trapped protons were thought to impose great effects on the apparent diffusion coefficient determined with potential step methods. Motupally and co-workers[13] found continuous changes of D with SOC using ac impedance and proposed a homogeneous solid solution model. In that model, the SOC dependent diffusion coefficient was described by an equation based on a mixing rule in terms of the root-mean-square displacement of the diffusion species. However, this model is not able to interpret our data. For example, Motupally's curve predicates a D change in about an order of magnitude in the SOC region 0−0.2. This change would cause corresponding large change (about 10 folds) in the slope of ln(i) vs t plot in potential step measurement, in conflict with our experimental data as shown in Figure 4 where almost perfect linear relationship kept over that region of SOC variation.

According to our experiments, a model must be able to accommodate the following major facts found in this work: (1) there are two distinctly different diffusion coefficients of the order 10^{-7} and 10^{-10} cm^{2}s^{-1}; (2) these two diffusion coefficients

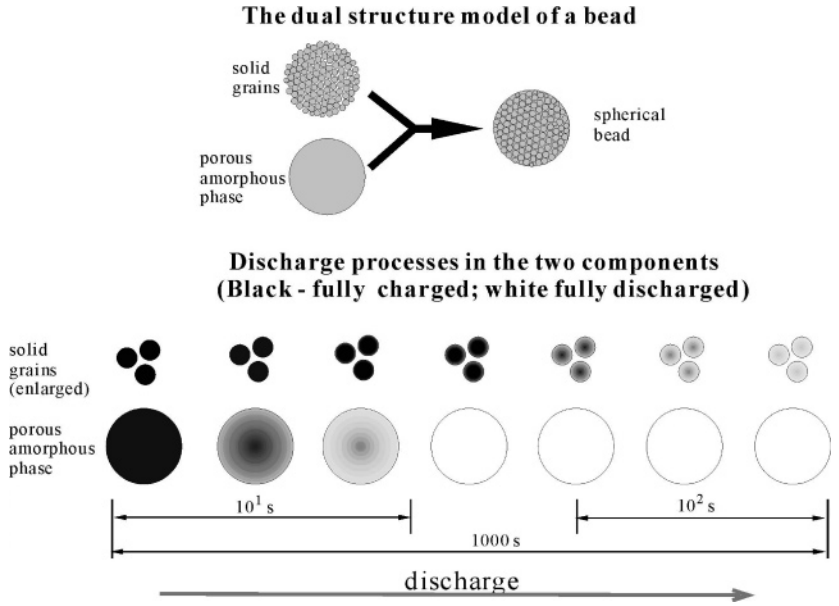

Figure 6. Schematic presentation of the dual structure model (upper) and the discharge processes in the two components (lower).

keep approximately constant with respect to SOC; (3) there is an additivity of the effective proton vacancy concentrations associated with the two diffusion coefficients, i.e., the sum of the two concentrations is approximately equal to the concentration converted from the discharge capacity of the bead, $C_\Sigma \approx C_T$. None of the existing models can meet these requirements.

We tentatively propose a dual structure model featuring small grains of the slow component packed in a matrix of the fast component, as shown in the upper part of Figure 6. The actual structure for each component is at present unknown and Figure 6 only gives a possible spatial relationship between the two components.

The discharge process of a spherical bead is schematically shown in the lower part of Figure 6. The state of charge is described by the gray level, with black representing the fully charged state and white the fully discharged state. During the cathodic potential step measurement, the fast component will be discharged quickly because of its large diffusion coefficient. In the short initial period of potential step measurement the contribution of the slow component is negligible because of its small diffusion coefficient so that the i vs $t^{-1/2}$ relationship is mainly governed by the fast component. According to the measured diffusion coefficient and the size of the bead, the fast component will be exhausted within a few tens of seconds. In the later time, the effective proton vacancy concentration of the fast component falls to essentially zero in the whole bead and the electrode response will be determined by the proton diffusion within the grains. After a sufficiently long time (about 200 s in Figure 4) the current response will become describable by eq 2A for individual grains. The recorded current is the summation of all the grains. If the grains are assumed uniform in size, a perfect straight line is expected for the plot of logarithmic current vs time. In experiments, the linearity was found fairly good, implying that the grain size was approximately uniform.

3.3.2. Apparent and Intrinsic Values of D and C. In the calculation of the C and D values shown in Table 1, the equations used (eqs 1A through 2A-b) are based on a homogeneous model. In the framework of the dual structure model, the physical meaning of thus obtained C and D values should be reconsidered. The D values shown in Table 1 are not intrinsic for either the fast or the slow component but are some kinds of apparent values. In this section we shall deduce the relationship between the apparent values and the intrinsic ones.

(A) *The Apparent and Intrinsic Values for the Slow Component.* According to the dual model, the long-term current response in the potential step measurement is determined by the proton diffusion in the grains. When eqs 2A-a and 2A-b are used to calculate the D and C values for the grains, the radius of the grain, r_g, instead of the radius of the bead, r_b, should be used. However, the D_s and C_s values shown in Table 1 were obtained by taking r_b for r. Therefore, these values are not intrinsic for the grains and only apparent values for the slow component. Because the size of the grain is unknown, it is impossible to obtain the intrinsic D and C values for the time being. Nevertheless, if we define a radius ratio of the bead to the grain, m, and the volume fraction of the slow component in the bead, f, simple relations can be found between the apparent and intrinsic values.

From eq 2A-b, it is straightforward that the intrinsic diffusion coefficient in the grain, D_g, is smaller than the apparent value D_s by a factor of m^2

$$D_g = D_s\, m^{-2} \tag{5}$$

If the grain had a diameter in the range of 50−100 nm, D_g should be on the order of 10^{-14} cm^2 s^{-1}.

It can be proved that the intrinsic concentration of effective proton vacancies in grains, C_g, is related to the above deduced apparent concentration C_s by a simple equation (see the Appendixes):

$$C_s = f C_g \tag{6}$$

Equation 6 indicates that the apparent value C_s is the concentration for the slow component averaged over the whole bead volume.

(B) The Apparent and Intrinsic Values for the Fast Component. Similar to the case of slow component, the apparent concentration of the fast component C_f is related to the intrinsic concentration of effective proton vacancies in the matrix, C_m, via the volume fraction:

$$C_f = C_m(1 - f) \tag{7}$$

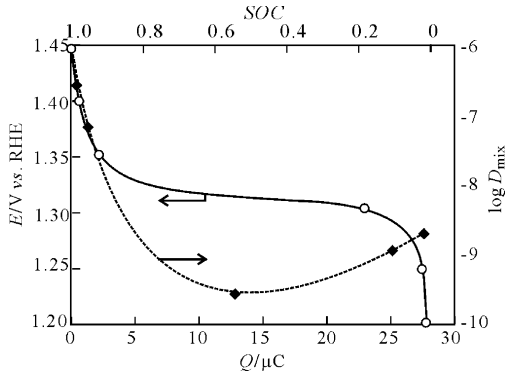

Figure 7. D_{mix} obtained in stair-wise discharge.

As well-known, the apparent diffusion coefficient of a continuous phase filling in a porous body, D_{app}, is related to the bulk diffusion coefficient of the continuous phase, D_0, through a simple equation

$$D_{app} = D_0(1 - f)/\beta^2 \tag{8}$$

where $(1 - f)$ is the volume fraction of the continuous phase in the porous body and β^2 is a parameter reflecting the zigzag path of the pores and for a pile of balls β^2 is about 3.

The relationship of the apparent diffusion coefficient (D_f) and intrinsic diffusion coefficient (D_m) for the fast component is an analogue to eq 8:

$$D_f = D_m (1 - f)/\beta^2 \tag{9}$$

If $f = 0.7$, then $D_m = 10D_f$, i.e., on the order of 10^{-6} cm^2 s^{-1}.

3.4. Partially Discharged Samples. In the above sections, the long-term response current was assumed to be predominantly contributed from the slow component while the initial response current mainly from the fast component. Both assumptions are valid for fully charged beads. For partially discharged beads, however, the first assumption (about the long-term response) remains valid, but the second one (about the short term response) does not. In general, the initial response current is the sum of the currents from the two components. In this case, the D value deduced from eq 1A will be a mixed value of C_s and C_f (see Appendixes):

$$D_{mix} = [xD_f^{1/2} + (1 - x)D_s^{1/2}]^2 \tag{10}$$

where x is the concentration fraction of fast component, i.e. $x = C_f/(C_f + C_s)$. As pointed above, the two components differ kinetically in discharge. Besides, they may also slightly differ from each other thermodynamically. As a result, x will not only change with SOC but change with SOC in different versions, depending on the way of discharge. Therefore, it can be expected that the D_{mix} value deduced from the initial current response will be SOC dependent, and the SOC dependence of D_{mix} observed by different researchers may not be the same. This prediction is supported by the results of stairswise potential step measurements shown in Figure 7. In this experiment, a fully charged bead was imposed a series of potential steps of 50 mV amplitude. After each potential step the response current was recorded for the first 1000 s but the destination potential was held for an hour to establish an equilibrium needed for the next potential step measurement. The SOC dependence of D_{mix} deduced from initial response is in qualitative agreement with that reported by Motupally and co-workers[13] except for the slight rise in low SOC region. This slight rise may be explained by nonmonotonic decrease of x with SOC.

3.5. Rationalization of Reported *D* Values. On the basis of the dual structure model, the widely scattered D values reported in the literature can be largely rationalized. For better comparability, only the D values obtained with cathodic potential step method on similar samples are compared. The samples to be compared include cathodically precipitated films and spherical beads. Spherical nickel hydroxide is produced by precipitation method and is, therefore, expected to have structure and property similar to those of the cathodically precipitated films. In contrast, the anodically formed films on nickel substrate may be different and is therefore not to be considered here. Anodic potential step may suffer from the interference caused by oxygen evolution and, therefore, the relevant data are not to be compared here either.

3.5.1. SOC Dependent vs SOC Independent D Value. First of all, we shall explain why some authors reported SOC independent D while others reported SOC dependent D. According to the dual model, in the long-term response to a potential step the current is governed by the diffusion in the slow component (the grains) regardless of the value of SOC. Therefore, the D values deduced from the long-term current response should be independent of SOC. This prediction was proved in our experiment. (The relevant data are not shown in this paper.) In contrast, if the initial response current is used to deduce the diffusion coefficient, thus obtained D will be a mixed one in nature (eq 10) and change with SOC.

The above predictions were in agreement with our experimental data (Figure 7) and literature data as well. Kim and coworkers[12] stepped potential from various starting points (0.45−0.6 V vs Hg/HgO, corresponding to different SOC) to 0.1 V and found the D deduced from the long-term current response being $3-4 \times 10^{-9}$ cm^2 s^{-1}, which are independent of SOC as predicted by the dual model. Yoon and Pyun[8] used both long and initial responses of potential step measurements to deduce D. The D values they deduced from the long-term current were round 3×10^{-12} cm^2 s^{-1}, essentially independent of the cathodic destination potential. On the other hand, the D values from the initial response (up to 10 s) changed from 10^{-10} to 10^{-8} cm^2 s^{-1}, depending on the potential step ranges.

3.5.2. Sample Size Effect on the D Value Deduced from Long-Term Current. When only the D values deduced from long-term current response are compared, the reported data scattering is still very large. According to the dual model, this scattering can be attributed in part to the difference in sample size.

To calculate the D value from the long-term current response using eq 2, a known r value is needed. According to the dual structure model, the rate determining process is the proton diffusion within the grains, the radius of the grain instead of the sample bead should be used in eq 2. Obviously, if the samples have exactly the same structure and properties, the experimental slope of ln(i) vs t plot, which is D/r^2, will be the same but thus deduced D value will strongly depend on size of the bead. Because the long-term current equation for planar films is similar to eq 2, this discussion is also applicable to film samples. Therefore, D/δ^2 values are expected to be less scattered than D. This deduction is supported by the data given below.

MacArthur[10] obtained 4.6×10^{-11} cm^2 s^{-1} from film samples about 0.55 μm thick. Yoon and Pyun[8] reported 3×10^{-12} cm^2 s^{-1} based on film samples of thickness ranging 0.5−0.8 μm. Ta and Newman[7] made very thin films (20−40 nm thick) on TIO coated glass plates and found 3.4×10^{-13} cm^2 s^{-1}. Kim

and co-workers[8] reported $3-4 \times 10^{-9}$ cm^2 s^{-1} from single beads of radius 15 μm measurements. In the present work the average D from long-term current response was 6.0×10^{-10} cm^2 s^{-1} with average $\delta = 15.8$ μm. The statistics on these five works produced an average logarithmic (D/cm^2 s^{-1}) -10.44 ± 1.70 and average (D/δ^2 s^{-1}) -2.7 ± 0.76. It can be seen that the data scattering is reduced from 3.4 to 1.5 orders of magnitude by correcting for the difference in macroscopic dimension, implying that the real difference in proton diffusion coefficient between these works is not as large as they appeared to be.

3.5.3. SOC Dependence of the D Values Deduced from Initial Current. According to the dual structure model, the D deduced from initial current is sensitive to SOC (eq 10) and the large value characteristic for the fast component can be obtained only if the sample is fully charged and the initial current in a sufficiently short time is used. Because of very quick exhaustion of the fast component, if the initial current over a relatively long duration is used for deducing D, a mixed value D_{mix} much smaller than D_f would result.

The present work found 1.8×10^{-7} cm^2 s^{-1} for fully charged beads while Yoon and Pyun[8] reported about 1×10^{-8} cm^2 s^{-1} for fully charged deposit films. The difference in D between the two works may be attributed at least in part to the difference in sampling time (1 s in our work vs up to 10 s in Yoon's work). We also found that a small D (on the order of 10^{-9} cm^2 s^{-1}) would be obtained if the current in the first 10 s instead of 1 s was used for the semi-infinite diffusion equation (eq 1A) even for a fully charged bead. The above analysis and experimental data both indicate that a part of controversy over the D values in the literature should stem from the ignorance of the SOD dependence for the apparent D deduced from the initial response current.

3.6. Preliminary Verification of the Dual Structure with AFM and SEM. In an attempt to verify the dual structure model by morphological observations, AFM and SEM were used. In Figure 8, parts A, C, and F are AFM images of the cross section for three different spherical hydroxide beads. All of them show submicrometer structures which are roughly spherical and uniform in size, in agreement with the assumption of grains in the dual structure model. Though the grain size is approximately uniform in a single bead, it varies from sample to sample. For example, the grain diameter is about 100 nm in picture A while it is below 50 nm in the other two pictures.

The AFM result is supported by SEM. Figure 8, parts D and E, are SEM images taken at exactly the same area of the AFM image shown in Figure 8F. Because the sample is electronically insulating, SEM was taken after Au sputtering. Figure 8D shows big features such as scratches and mosaic due to sputtered nano Au particles but reveals no sign for grains. After digital blurring to remove the mosaic and enlarging the contrast, Figure 8E was obtained, which well repeats the grains features found by AFM. The vertical lines in Figure 8 are of precisely the same length to indicate the correspondence between AFM and SEM for a number of selected grains. On the whole the correspondence should be regarded satisfactory. Both AFM and SEM images give a picture of "densely packed potatoes buried in soil", in support of our dual structure model.

It should be pointed out that the internal structures of the fast and slow components are not yet clear. For example, the crystalline structure revealed by XRD data is not included in the model. The grains may be single crystals or tightly packed single crystals. There were two papers[14,16] found in the literature reporting the influence of crystal size on the proton diffusion coefficient in nickel hydroxide. The two works agreed that higher D values were correlated to smaller crystal sizes, but they differed largely in the extent to which D depends on the crystal size. Nevertheless, their finding about the D dependence on crystal size is in qualitative agreement with our dual structure model. On the other hand, the diffusion profile development shown in Figure 6 for the fast component is not the only possibility either. For example, the fast component might be composed of very fine particles of nickel hydroxide (in the size of nanometers) and the very quick current decay in the first few seconds of potential step measurement might be due to the diffusion within these fine particles which are present in very large number in the sample. The different assumptions for the identity of the two components will affect the physical meaning and value of the so-called intrinsic D discussed in preceding sections. However, the main conclusions given in section 3.5 are independent of the detailed assumption of the each component and will remain valid in general.

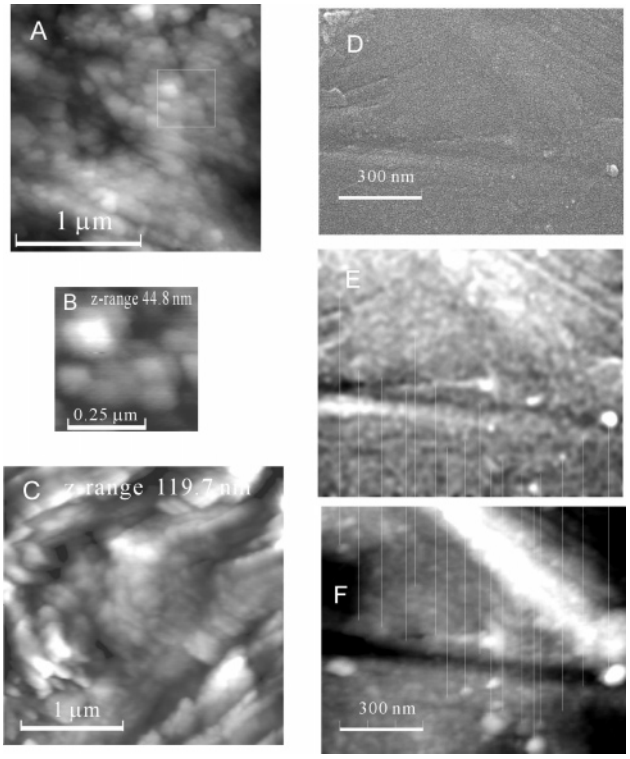

Figure 8. AFM and SEM images of internal structure for spherical nickel hydroxide. Parts A, C, and F are AFM images for different samples and part B is a higher resolution AFM for the marked area in A. Parts D and E are SEM images before and after digital processing, respectively. The vertical lines indicate the corresponding features between SEM (E) and AFM (F). The z range for image F is approximately 150 nm.

4. Conclusions

By using a microcavity electrode device, the potential step measurement was successfully applied to single beads of spherical nickel hydroxide. The proton diffusion coefficient (D) and the effective proton vacancy concentration (C) in the charged bead were deduced from the discharge current response. From the initial and long-term current responses two sets of concentrations and diffusion coefficients were obtained and interpreted by the coexistence of fast and slow diffusing components in a dual structure model.

On the basis of the model, the huge differences (spanning about 6 orders of magnitude) in the D values reported in the literature as well as the controversy over SOC dependence of

D can be largely rationalized. The essential reason for the apparently serious disagreement in reported D values is the fact that there coexist two components with very different diffusion coefficients and the different reported D values were governed by the two components in different ways depending on the details of experiments and data processing. The highest reported D values (roughly on the order of 10^{-7} cm^2 s^{-1}) are characteristic of the fast component and can only be obtained from a short initial response in potential step measurements for fully charged samples. On the other hand, the lowest reported D values are characteristic of the slow component and are obtained from the long-term current response. The D values from the long-term current are independent of SOC but depend on the sample size taken in the calculation, for sample sizes round 50 nm these values are likely on the order of $10^{-13}-10^{-14}$ cm^2 s^{-1}. When the initial currents are used to deduce D for partially discharged samples, the result would be SOC dependent values between the above-mentioned high and low extremes. In light of the dual model, the real difference in proton diffusivity among the samples reported by different researchers are actually not as large as they appeared.

Acknowledgment. This work was supported by the Natural Science Foundation of China (NSFC No. 20073223) and the State Key Laboratory of Physical Chemistry for Solid surfaces at Xiamen University (Project No. 200206). The authors thank Mr. Guoqing Cao, secretary of Chinese Association of Batteries, for collecting samples. Thanks are also to the suppliers of the samples.

Appendix 1. Deduction of Equations 5 and 6

In the long-term response of potential step measurement, the recorded current is the sum of the currents from all the grains in a single bead. Assuming the grains have approximately uniform size and have radius r_g, the current from a single grain can be expressed by eq 2A:

$$i_g = 8nF\pi r_g D_g C_g \exp[(-\pi^2 D_g/r_g^2)t] \quad \text{(a)}$$

If the total volume of all the grains in a bead accounts for a volume fraction f and the radius ratio of the bead to grain is $r_b/r_g = m$, the number of grains in a bead is

$$N_g = fm^3 \quad \text{(b)}$$

and the recorded current is

$$i = N_g i_g \quad \text{(c)}$$

Substituting eqs a and b into eq c results

$$i = fm^3\, 8nF\pi r_g D_g C_g \exp[(-\pi^2 D_g/r_g^2)t]$$

This equation can be rewritten as

$$i = 8nF\pi\, m r_g\, m^2 D_g f C_g \exp[(-\pi^2 m^2 D_g/m^2 r_g^2)t] \quad \text{(d)}$$

Without the dual structure model, the radius of the bead r_b is to be substituted into eq 2A to correlating the recorded current with the apparent value D_s and C_s:

$$i = 8nF\pi r_b D_s C_s \exp[(-\pi^2 D_s/r_b^2)t] \quad \text{(e)}$$

Compare eq c with eq d, remembering that $r_b = mr_g$, and eqs 5 and 6 are obtained:

$$D_s = m^2 D_g \quad (5)$$

$$C_s = fC_g \quad (6)$$

Appendix 2. Deduction of Equation 10

In the short-term response to a potential step, the recorded current is in general the sum of the currents contributed from the fast and slow components. This problem can be treated in terms of either apparent or intrinsic parameters. Identical results will be reached, but the approach using apparent D and C is simpler and therefore given below.

According to eq 1A, the short term currents from the fast and slow components are

$$i_f = 4F\pi r_b^2 D_f C_f [(\pi D_f t)^{-1/2} - r_b^{-1}] \quad \text{(f)}$$

$$i_s = 4F\pi r_b^2 D_s C_s [(\pi D_s t)^{-1/2} - r_b^{-1}] \quad \text{(g)}$$

The recorded current is the sum of eqs f and g; after rearrangement it can be expressed as

$$i = 4F\pi^{1/2} r_b^2 [D_f^{1/2} C_f + D_s^{1/2} C_s] t^{-1/2} - 4F\pi r_b [D_f C_f + D_s C_s] \quad \text{(h)}$$

Introducing the concentration fraction of fast component x,

$$x = C_f/(C_f + C_s) \quad \text{(i)}$$

For simplicity, the difference between $(C_f + C_s)$ and the total effective proton vacancy concentration C_T can be neglected and eq h can be rewritten into

$$i = 4F\pi^{1/2} r_b^2 C_T [xD_f^{1/2} + (1-x)D_s^{1/2}] t^{-1/2} - 4F\pi r_b [xD_f + (1-x)D_s] \quad \text{(j)}$$

Traditionally, the diffusion coefficient is deduced from the slope of experimental i vs $t^{-1/2}$ plot and a value for C, which is considered to be the total concentration of effective proton vacancies C_T, using eq 1A. By comparing eq 1A with eq j, eq 10 is obtained:

$$D_{mix} = [\, xD_f^{1/2} + (1-x)D_s^{1/2}]^2 \quad (10)$$

References and Notes

(1) Linden, D.; Ed. *Handbook of Batteries*; McGraw-Hill: New York, 1995.
(2) Weidner, J. W.; Timmerman, P. *J. Electrochem. Soc.* **1994**, *141*, 346.
(3) Motupally, S.; Streinz, C. C.; Weidner, J. W. *J. Electrochem. Soc.* **1998**, *145*, 29.
(4) Paxton, B.; Newman, J. *J. Electrochem. Soc.* **1996**, *143*, 1287.
(5) Srinivasan, V.; Weidner, J. W.; White, R. E. *J. Solid-State Electrochem.* **2000**, *4*, 367.
(6) MacArthur, D. M. *J. Electrochem. Soc.* **1970**, *117*, 422.
(7) Zhang, C.; Park, S. *J. Electrochem. Soc.* **1987**, *134*, 2966.
(8) Yoon, Y.; Pyun, S. *Electrochim. Acta* **1997**, *42*, 2465.
(9) Briggs, G. W. D.; Snodin, P. R. *Electrochim. Acta* **1982**, *27*, 565.
(10) MacArthur, D. M.*J. Electrochem. Soc.* **1970**, *117*, 729.
(11) Ta, K. P.; Newman, J. *J. Electrochem. Soc.* **1998**, *145*, 3860.
(12) Kim, H.-S.; Itoh, T.; Nishizawa, M.; Mohamedi, M.; Umeda, M.; Uchida, I. *Int. J. Hydrogen Energy* **2002**, *27*, 295.
(13) Motupally, S.; Weidner, J. W. *J. Electrochem. Soc.* **1995**, *142*, 1401.
(14) Watanabe, K.; Kikuoka,T. *J. Appl. Electrochem.* **1995**, *25*, 219.
(15) Carslaw, H. S.; Jaeger, J. C. *Conduction of heat in Solid*, 2nd ed.; Clarendon Press: Oxford, England, 1986; p 233.
(16) Gille, G.; Albrecht, S.; Meese-Marktscheffel, J.; Olbrich, A.; Schrumpf, F. *Solid State Ionics* **2002**, *148*, 269.